Available online at www.sciencedirect.com
ScienceDirect
Journal of the European Ceramic Society 27 (2007) 1419–1424
www.elsevier.com/locate/jeurceramsoc

Improving strength by controlling segregation in liquid phase sintered aluminium nitride ceramics

A. Klimera [a], F. Raether [a,*], J. Ruska [b]

[a] *Fraunhofer-Institut Silicatforschung ISC, Neunerplatz 2, D-97082 Würzburg, Germany*
[b] *CeramTec AG, Lorenzreuther Str. 2, D-95615 Marktredwitz, Germany*

Available online 6 June 2006

Abstract

SEM investigations on liquid phase sintered AlN ceramics showed segregation of the liquid phase. The liquid phase concentrated in clusters of some tens of micrometers in diameter. Crack deflection was observed in the vicinity of the clusters indicating high thermal stresses which could impair strength and reliability of the ceramics. Therefore, a thermodynamic model based on interface and grain boundary energies was established. With it the parameters were identified which caused segregation of the liquid phase during sintering. Due to the high contrast in thermal conductivity between liquid phase and AlN, wetting properties of the liquid phase could be determined indirectly by measuring the thermal conductivity of the ceramics at temperatures between 1600 and 1850 °C. In situ measurements of shrinkage and thermal conductivity were performed using a Thermooptical measuring device (TOM). With it a sintering process was developed which led to a homogeneous microstructure without segregation. An increase of flexural strength by 25% and of Weibull modulus higher than 80% was achieved.

Keywords: Sintering; Defects; Mechanical properties; Nitrides; Substrates

1. Introduction

An increasing power density of the electronic devices demands an ever increasing efficiency of their thermal management. The thermal resistance of the ceramic substrates used in heat sinks is inversely proportional to their thickness. Therefore, cooling efficiency can either be enhanced by increasing the thermal conductivity of the ceramic or by decreasing thickness of the substrates. The latter requires an increase in material strength and reliability since the strength of the substrates scales by the square of their thickness.

Aluminium nitride ceramics are used as substrates for heat sinks in electronic industry because of their good thermal conductivity and because of their low thermal expansion coefficient which matches to that of silicon. During pressureless sintering of AlN ceramics sintering additives are used which form a liquid phase at high temperatures and help in purification of the AlN grains during their solution and reprecipitation. The mechanism was described in detail by Virkar and co-workers.[1] With the common sintering aid Y_2O_3 Yttrium-aluminate phases are formed from the reaction with alumina which is partly located on the surface of the AlN particles and partly dissolved in the AlN.[2] The Yttrium-aluminate formation starts at temperatures as low as 1100 °C.[3] There are three different Yttrium-aluminate phases: $Y_3Al_5O_{12}$, $YAlO_3$, and $Y_4Al_2O_9$.[4] The eutectic with the lowest melting point lies in the $YAlO_3$–$Y_4Al_2O_9$ two phase field. Its melting point is 1800 °C in the pure system[4] and 1600 °C in presence of AlN.[3] The oxygen activity within the liquid phase has to be sufficiently low to limit the oxygen concentration in the reprecipitated AlN. It decreases with increasing concentration of Y_2O_3 within the liquid phase.[1] Yet with increasing concentration of yttria the thermal conductivity of the AlN ceramics passes a maximum. This is caused by an increasing fraction of secondary phase which has a very low thermal conductivity itself.[5]

The fracture strength of AlN ceramics which was reported in literature varies between 300 and 500 MPa. It is believed that there is a strong influence of the measuring procedure on the measured strength and only part of the variation is caused by differences in the ceramics. Different concepts were tested to improve mechanical properties of AlN ceramics. Using additives which do neither dissolve in the liquid phase nor in AlN a dispersion strengthening was proposed.[6] This can be supported by grain growth inhibition of AlN by the dispersed phase. (Phases

* Corresponding author.
E-mail address: raether@isc.fraunhofer.de (F. Raether).

0955-2219/$ – see front matter © 2006 Elsevier Ltd. All rights reserved.
doi:10.1016/j.jeurceramsoc.2006.04.098

which are stable during sintering of AlN ceramics were identified by Reetz using thermodynamic calculations.[7]) Other strengthening concepts which were used with non oxide ceramics consider the stress distribution in the ceramics. By introducing compressive stresses in the matrix phase a higher bending strength was achieved.[8] Another way to improve the mechanical properties of ceramics is to avoid an inhomogeneous microstructure.[9] Microstructural flaws as pores, cracks and clusters of Yttrium-aluminate are decreasing the bending strength.

2. Experimental procedure

Samples were prepared from a high purity AlN powder (Tokuyama Soda Co., Grade H). Mean particle size of the powder (d_{50}) was 0.4 μm. Its oxygen content was 0.7% where 0.5% was situated on the particle surface and 0.2% was dissolved in the AlN lattice.[2] As sintering aid Y_2O_3 powder with a mean particle size of 0.9 μm was used (H.C. Starck). Samples were made in a laboratory scale after drying the powder mixture in a vacuum drying chamber (12 h at 250 °C). The concentration of Y_2O_3 was matched to the oxygen content of the respective green samples to ensure that the secondary phase composition was within the $YAlO_3$–$Y_4Al_2O_9$ two phase region. The powder mixture was homogenised in a rotary drum grinder using 0.5% butylamine as a dispersing agent, nylon coated steel balls and a nylon or polyethylene container. The powder was sieved through a 100 μm screen, filled into silicon rubber moulds and cold isostatically pressed at a pressure of 250 MPa to cylinders of 11 mm diameter and 30 mm height. Green density was 60% of theoretical density. The lab route was used for making thick samples which were required for the in situ measurements (see below). Other AlN samples were made by a tape casting process which is described in more detail in[10] and which was also used for the industrial production of the AlN ceramics.

Sintering was done in resistance heated graphite furnaces. The furnace atmosphere was pure nitrogen. In the graphite furnaces the AlN was protected by closed caskets against reducing gas species from the furnace atmosphere.[11] In situ measurements were done during sintering of small disc shaped AlN samples (11 mm diameter and 1.4 mm thick) in a graphite heated furnace. A special thermooptical measuring device (TOM) was used for this purpose which was described in more detail before.[12] Pure nitrogen (5.0) with a flow of 2 l/min was used for the in situ measurements. Since optical access to the sample was necessary a closed casket could not be used and a careful control of the furnace atmosphere was required to prevent reduction of the liquid phase. For this purpose gas sensors for CN and CO have been installed in the exhaust gas of the furnace. The CN and CO concentrations were kept below, respectively 100 and 700 ppm. This was sufficient to obtain sintered AlN samples of full density and similar secondary phase composition as in the closed caskets.

The TOM enables a simultaneous measurement of sintering shrinkage and thermal diffusivity. Sintering shrinkage was measured by an optical dilatometer with a resolution of 1 μm.[13] Thermal diffusivity was measured by the laser flash technique.[12] Fractional density was calculated from sintering shrinkage curves by correcting for the thermal expansion and by interpolating between the green density and the measured final density of the samples.[13] A scaled thermal conductivity was calculated from the measured thermal diffusivity α by dividing by the corresponding values of a dense AlN sample measured at the same temperature and by multiplying with density ρ:

$$\lambda_{\text{scaled}} = \frac{\rho_{\text{Sinter}}(T)}{\rho_{\text{Dense}}(T)} \frac{\alpha_{\text{Sinter}}(T)}{\alpha_{\text{Dense}}(T)} \quad (1)$$

Sintered density of the AlN samples was measured using the Archimedian method. Thermal conductivity at room temperature was calculated from thermal diffusivity α measured by the laser flash technique, density ρ and specific heat capacity c_p according to

$$\lambda = \rho c_p \alpha \quad (2)$$

An average value of 738 J/(kg K) was used for the specific heat capacity which was determined by dynamic scanning calorimetry (Perkin-Elmer, DSC 2). The microstructure of the samples was investigated by scanning electron microscopy at fracture surfaces or polished sections (Hitachi, S800).

Strength of the samples has been measured by a three-point bending test and by a ball-on-ring test,[18] respectively. For the three-point bending test sample size was 25.4 mm × 15 mm × 0.63 mm and the distance between the bearings was 20 mm. For the ball-on-ring test, sample size was Ø 13 mm × 0.5 mm and the inner ring diameter was 7.7 mm.

3. Experimental results and discussion

Thermal diffusivity of a sintered AlN sample was measured at different temperatures. It was scaled by the thermal diffusivity of an AlN sample whithout liquid phase measured at the same temperature (Fig. 1). (Liquid phase of this sample was completely extracted by sintering at 1900 °C for 18 h.) Thermal conductivity of a sintered AlN sample with liquid phase was nearly 100% of that of the pure AlN sample at 1600 °C. It decreased with increasing temperature and increased again if the temperature was decreased. The thermal diffusivity of the liquid phase was measured to $0.80 \pm 0.06\ \text{mm}^2/\text{s}$ between 1500 and

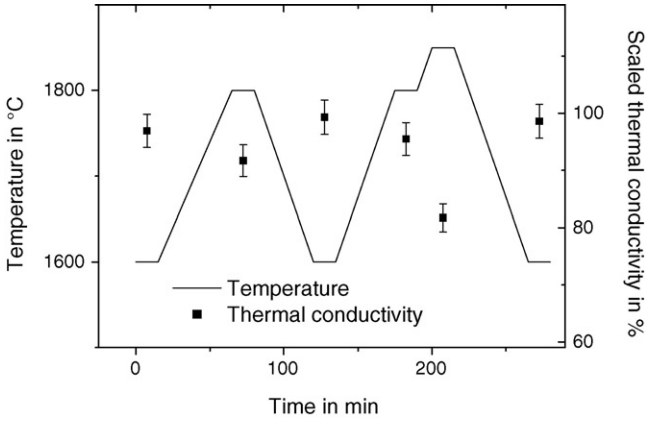

Fig. 1. Scaled thermal conductivity of a sintered AlN sample measured at different temperatures.

1700 °C (measured in BN-crucible by the laser flash technique). Composition of the liquid phase was $YAlO_3$–$Y_4Al_2O_9$ eutectic melt with 12 mol% AlN.[3] (Thermal diffusivity was determined by inverse modelling of the temperature curve using a finite difference method and considering also the heat flow through the crucible.) The thermal diffusivity of the melt is to be compared to a much higher thermal diffusivity of a pure AlN sample of $5.8 \pm 0.04\,mm^2/s$ in this temperature range. Therefore, the reversible change of scaled thermal conductivity (compare Fig. 1) was attributed to a decrease of dihedral angle with temperature. This decrease led to a reduction in the AlN–AlN grain boundary area and to a higher thermal resistance at the grain contacts. The in situ measurement confirms previous investigations where a decrease of dihedral angle with temperature was derived indirectly from microstructure investigations at room temperature using different cooling rates.[14]

Fig. 2a shows the fractional density of AlN green samples with 3% Y_2O_3 determined from a TOM measurement of sintering shrinkage with different heating rates and subsequent constant temperature heating at 1800 °C. Shrinkage began at 1350 °C. At 1580 °C there was a sharp bend in shrinkage rate. The fractional density varied at this point between 67% and 71% depending on the heating rate. This behaviour cannot be explained on the basis of usual sintering models. (Note that the corresponding temperature was close to the temperature of liquid phase formation measured in these AlN ceramics.[3]) Full density was achieved after about 1 h holding time. Fig. 2b shows the scaled thermal conductivity determined from a simultaneous measurement of thermal diffusivity. The course of the curves was similar to that of the fractional density. Mechanisms can be seen more clearly from a plot of thermal conductivity versus density (Fig. 3). There was no significant influence of heating rate on those curves. In the initial sintering stage there was neither a steep increase of thermal conductivity with density as was observed for systems where surface diffusion was relevant[15] nor was the slope near zero as was expected if initial densification were caused only by particle rearrangement (particle rearrangement increases density but not sintering neck size which is most important for thermal conductivity in the initial sintering stage[15]). In the final sintering stage thermal conductivity still increased while full density was already achieved resulting in a vertical slope at the end of the curves. This was indicated by the arrow in Fig. 3 and was explained by an increase in dihedral angle during the hold period (compare previous paragraph). The dihedral angle Θ is defined by the ratio between the specific AlN–AlN grain boundary energy γ_{GB} and the interface energy of AlN and liquid phase γ_{SL} according to

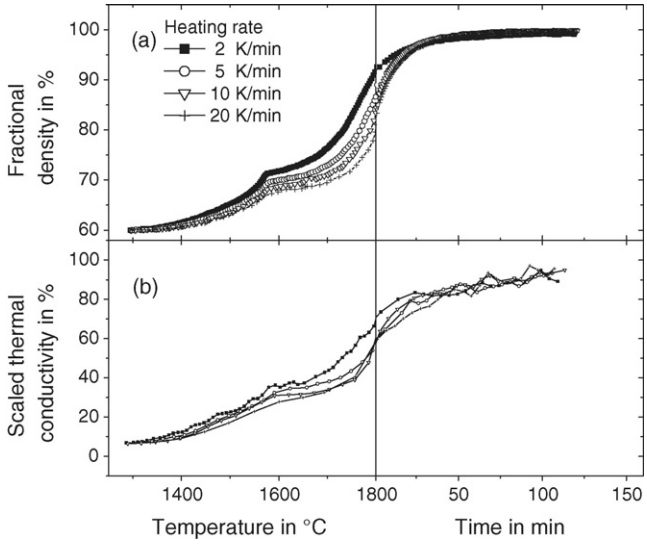

Fig. 2. Fractional density (a) and scaled thermal conductivity (b) during sintering of AlN ceramics with different heating rates.

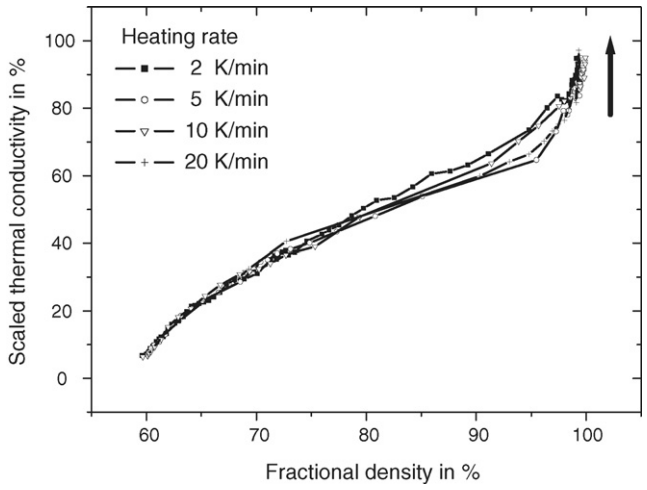

Fig. 3. Scaled thermal conductivity vs. fractional density during AlN sintering.

$$\cos\left(\frac{\Theta}{2}\right) = \frac{\gamma_{GB}}{2\gamma_{SL}} \tag{3}$$

Therefore, an increase in dihedral angle can be caused as well by a decrease in grain boundary energy γ_{GB} as by an increase in interface energy γ_{SL}. A large variation of dihedral angles measured at polished sections at room temperature between 60 and 110 °C was found in the AlN ceramics. This shows that grain boundary energy is largely affected by the mutual crystalline orientation of the grains. Therefore, during final stage sintering of AlN ceramics grain growth could have occurred where the grain boundaries with lower energy were preferred leading to a decrease of average grain boundary energy. But also an increase of γ_{SL} is expected since the composition of the liquid phase was changed during the hold time (due to an increase of Al_2O_3 concentration originating from oxygen impurities dissolved in the AlN grains and a decrease of AlN concentration originating from a decrease of AlN activity caused by the reduced surface curvature of the growing AlN grains[3]).

Fig. 4a shows a SEM image of a polished AlN sample which was heated by a standard program using a constant heating rate of 5 K/min up to 1850 °C with a hold for 45 min. The secondary phase can be distinguished from AlN by its brighter contrast. It was distributed unevenly in clusters of 20–50 μm diameter. SEM images from fracture surfaces of these ceramics showed crack deflection in the vicinity of the clusters indicating high thermal stresses which could impair strength and reliability of the ceramics. Similar segregation phenomena were observed

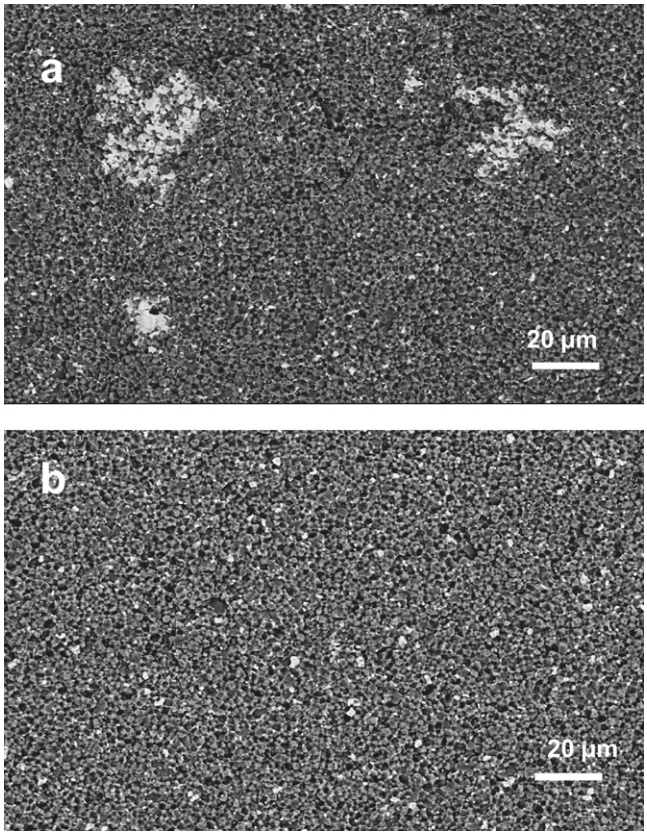

Fig. 4. SEM image showing segregation of liquid phase in conventional AlN ceramics (a) and homogenous distribution as a result of optimized sintering program (b).

in the tape cast samples. Therefore, a thermodynamic model was derived which could explain the segregation of the liquid phase.

The model is based on a three-dimensional lattice with a tetrakaidecahedral unit cell. The tetrakaidecahedral unit cell describes best the final sintering stage since the number of nearest neighbours is 14 (resulting from 8 hexagonal and 6 quadratic faces, Fig. 5) and the corners of the tetrakaidecahedron are met by 4 edges each which is close to the structure of sintered materials.[16] Using the high symmetry of the unit cell only 1/48th of the cell volume was actually used for the simulations (Fig. 5) and subsequent Figs. 6b and 7 were constructed by the appropriate symmetry operations.

For given volume fractions of the two phases and given grain boundary and interface energies the structure with minimal energy was calculated by the program surface evolver.[17] It starts with a simple prescribed geometry which has the right cell symmetry and volume fractions. Each interface is composed of plane triangular facets defined by vertices. The vertices are moved after subsequent iterations according to an individual force vector. The force vector is calculated locally for each vertex from the tensions originating from the neighbouring vertices. Appropriate constraints were used to ensure that the cell symmetry was bewared during the minimisation. The mesh was successively refined ending up with about 100–200 vertices. Convergence was achieved after a total of about 100 iterations.

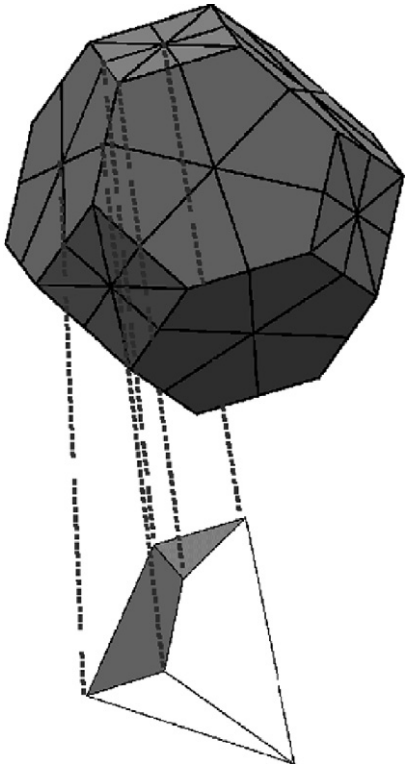

Fig. 5. Tetrakaidecahedral unit cell and the section actually used for surface minimisation.

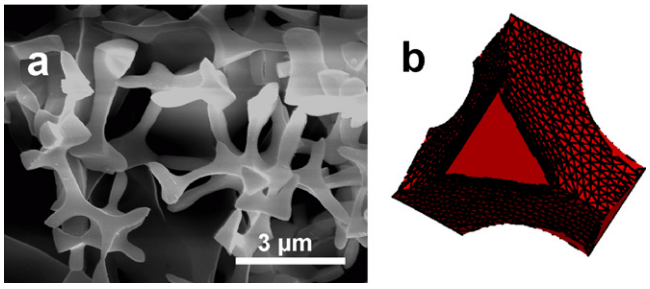

Fig. 6. Secondary phase (yttrium-aluminates) within AlN ceramics after removing the AlN by etching (a) and simulated shape of secondary phase situated at the corners of AlN grains (b) (volume fraction of liquid phase 5%, dihedral angle 60°).

Fig. 6b shows the equilibrium structure for the secondary phase obtained for a liquid volume fraction of 5% and a dihedral angle of 120°. The simulated structure was very similar to SEM images of the microstructure of the AlN ceramics which

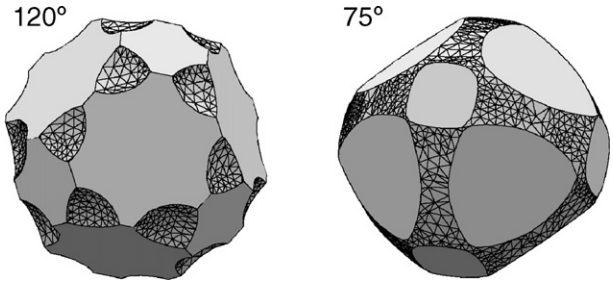

Fig. 7. Shape of AlN grains obtained after minimising the interface energy for a dihedral angle of 120° (a) and 75° (b) (volume fraction of liquid phase 5%).

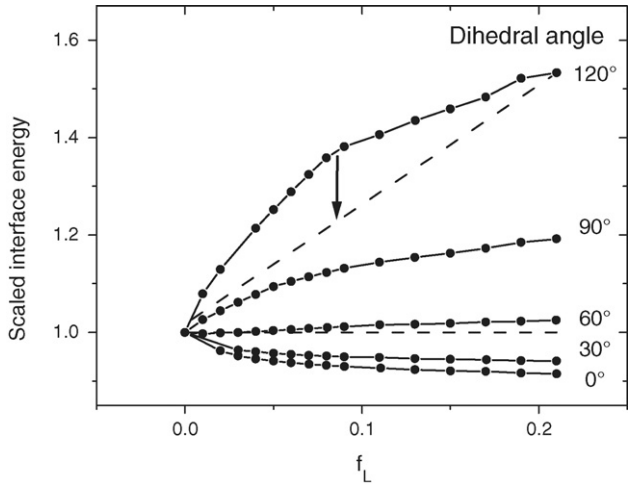

Fig. 8. Scaled interface energy for different dihedral angles vs. liquid volume fraction f_L (the arrow indicates possible decrease of interface energy by segregation).

were recorded after removing the AlN phase by etching with NaOH solution (Fig. 6a). The shape of the AlN grains drastically change by changing the dihedral angle (Fig. 7). With large dihedral angles the liquid phase is isolated at the grain corners whereas at smaller dihedral angles it is connected via the grain edges. A dihedral angle of zero leads to an entire wetting of the grain boundaries. The interface energy of the equilibrium structures was calculated by summing up the contributions from all interfaces within one unit cell including the grain boundaries. It was scaled by the interface energy of monophased tetrakaidecahedral solid grains of equal volume as within the two phase structure. Therefore, the scaled interface energy E_{scaled} approaches one if the volume fraction of the liquid phase f_L approaches zero. Fig. 8 shows the scaled interface energies for various dihedral angles as a function of the fraction of the liquid phase. The interface energy exceeds 1 if the dihedral angle becomes larger than 60°. Therefore, at dihedral angles above 60° the total interface energy of a two phase system can be reduced by a release of liquid phase at its surfaces which is well known for liquid phase sintering.[16] Moreover, the curves in Fig. 8 become convex at dihedral angles larger than 60° meaning that even a partial segregation within the two phase material will result in a smaller total interface energy. This can be seen by applying the lever rule which is well known from binary phase diagrams (Fig. 8). The energy decrease caused by segregation scales by the curvature d^2E_{scaled}/df_L^2 of the interface energy curves and by the difference in liquid fraction Δf_L which is achieved in the segregated regions. For dihedral angles below 60° the homogenous microstructure has the smallest energy and no segregation phenomena can occur.

Taking into account the increase of dihedral angle Θ with hold time and its decrease with temperature which were derived from the in situ measurements a time–temperature cycle was derived for the AlN ceramics which led to minimal segregation. Thereby the need for obtaining a high thermal conductivity had to be considered. The latter required solution and reprecipitation of a large fraction of the AlN since the oxygen impurities had to be removed from the lattice. According to the thermodynamic model described previously the dihedral angle was decreased by applying high temperatures and by carefully avoiding oversintering in this stage. On the other hand a large dihedral angle was desired in the final microstructure to avoid secondary phase as thermal resistance within the grain boundaries. So the temperature profile in the cooling stage after sintering had to be carefully designed, too. Altogether, a very homogenous microstructure was achieved after optimization of the sintering cycle (Fig. 4b) and a thermal conductivity of 180 W/mK was obtained. Three-point bending strength of the AlN ceramics increased from 390 to 500 MPa. Moreover, a very drastic increase from 12 to 22 of the Weibull modulus was obtained (Table 1).

Table 1
Bending strengths and Weibull moduli of AlN samples sintered by the standard procedure and sintered by the optimized time temperature cycle, respectively

	Ball-on-ring test[a] (MPa)	3-point bending strength[b] (MPa)	Weibull modulus[b]
Standard sintering	363 ± 48	392 ± 27	12
Optimized sintering	490 ± 37	495 ± 26	22

[a] Cold isostatically pressed samples.
[b] Tape cast samples (Weibull modulus derived from 3-point bending strength test data).

4. Conclusions

A considerable improvement of mechanical properties was obtained by changing the time–temperature cycle during liquid phase sintering of AlN ceramics. Very homogeneous microstructures could be produced and segregation between liquid phase and AlN was avoided. The optimization of the time–temperature cycle was based on a thermodynamic concept considering local minimisation of interface energies. The required material data were provided by special in situ measuring techniques. It is believed that this concept can also be applied to other liquid phase sintering systems where segregation phenomena occur.

Acknowledgements

The authors thank S. Beyer, R. Springer and N. Keidel for help with the measurements and G. Müller for valuable advice. They also gratefully acknowledge the financial support of German Science foundation (DFG) with contract Ra614/4.

References

1. Jackson, T. B., Virkar, A. V., More, K. L., Dinwiddie, R. B. and Cutler, R. A., *J. Am. Ceram. Soc.*, 1997, **80**, 1421.
2. Thomas, A. and Müller, G., *J. Eur. Ceram. Soc.*, 1991, **8**, 11.
3. Müller, G., Raether, F. and Jacobsen, L., In *Ceramics – Getting into the 2000s – Part B*, ed. P. Vincenzini. TechnaGroup, Florenz, Italy, 1999, p. 721.
4. Abell, J. S., Harris, I. R., Cockayne, B. and Lent, B., *J. Mater. Sci.*, 1974, **9**, 527.
5. Buhr, H. and Müller, G., *J. Eur. Ceram. Soc.*, 1993, **12**, 271.
6. Yun, Y. H. and Choi, S. C., *J. Mater. Sci.*, 1998, **33**, 707.
7. Reetz, *Z. f. Silikattechnik*, 1991, **42**, 298.
8. Lange, F. F., *J. Am. Ceram. Soc.*, 1980, **63**, 38.

9. Aldinger, F., *Keram. Zeitschrift*, 1988, **40**, 312.
10. Ruska, J. and Ernst, J., *Fortschrittsber. D. Dt. Keramischen Ges.*, 2004, **18**, 21.
11. Beyer, S., Brunner, D., Gottschalk, T., Jaennicke-Rößler, K., Leitner, G., Raether, F. *et al.*, In *Materials Week, Vol. 1*, ed. K. Kempter and J. Haußelt. Wiley–Vch, München, 1998, p. 11.
12. Raether, F., Hofmann, R., Müller, G. and Sölter, H. J., *J. Therm. Anal.*, 1998, **53**, 717.
13. Raether, F., Springer, R. and Beyer, S., *Mater. Res. Innovat.*, 2001, **4**, 245.
14. Kang, S.-J. K., Kim, K.-H. and Lee, S.-M., *Sintering Technology*. Dekker, New York, 1996, p. 221.
15. Raether, F., In *Sintering Science and Technology*, ed. R. M. German, G. L. Messing and R. G. Cornwall. Pennsylvania State University, 2000, p. 183.
16. German, R. M., *Sintering Theory and Practice*. John Wiley & Sons, New York, 1996.
17. Brakke, K., *Exp. Math.*, 1992, **1**, 141–165.
18. With, G. and deWagemans, H. H. M., *J. Am. Ceram. Soc.*, 1989, **72**, 1538–1541.